Int J Adv Manuf Technol (2016) 87:293–302
DOI 10.1007/s00170-016-8365-2

ORIGINAL ARTICLE

# A hybrid method for crackless and high-efficiency ultraprecision chamfering of KDP crystal

**Dongsheng Chen**[1,2] · **Jihong Chen**[1] · **Baorui Wang**[2]

Received: 30 September 2015 / Accepted: 13 January 2016 / Published online: 19 February 2016


**Abstract** To enhance the optical performance of the optics used in inertial confinement fusion (ICF), the edges of the large-sized KDP crystal need to be removed to form chamfered faces with high surface quality (RMS <5 nm). Fly cutting with single point diamond tool has been widely used to process potassium dihydrogen phosphate (KDP) to achieve extremely high surface quality. However, the depth of cut (DOC) of fly cutting is usually several microns, which results in very low machining efficiency for the chamfering of KDP crystal as the amount of materials to be removed is in the order of millimeter. To overcome this problem, this paper proposes a hybrid machining method by combining precision grinding with fly cutting to achieve crackless and high-efficiency ultraprecision chamfering of KDP crystal. In addition, a combined machine tool has been developed, and experiments have been carried out to determine the optimal machining procedures and verify the effectiveness of the proposed method. Experimental results show that the machining efficiency can be improved by nearly five times using the proposed method to produce the same machined surface quality as that of the traditional fly cutting process.

**Keywords** KDP crystal · Ultraprecision chamfering · Fly cutting · Precision grinding

✉ Jihong Chen
13308656728@189.cn

[1] School of Mechanical Science & Engineering of HUST, 1037 Luoyu Road, Wuhan, People's Republic of China

[2] Institute of Mechanical Manufacturing Technology, CAEP, 64 Mianshan Road, Mianyang, Sichuan, People's Republic of China

## 1 Introduction

Potassium dihydrogen phosphate (KDP) is a type of nonlinear optical crystal material. For example, it often used in the frequency converters and the electro-optical switches in the modern high energy laser directed energy weapons, the laser fusion system in the inertial confinement fusion (ICF) programs [1, 2]. The traditional KDP crystal used is shown in Fig. 1a. When laser light propagates through the KDP crystal, spontaneously scattered light can experience high gain across the transverse dimensions of the crystal, leading to energy loss from the main beam [3]. To reduce the energy loss, Barker et al. [4] proposed to remove the edges of the large-sized KDP crystal to form chamfers as shown in Fig. 1b. For the KDP crystal with a thickness of 12 mm, a chamfer with its dimension shown in Fig. 1c should be cut at each edge, corresponding to a total depth of cut of about 3 mm from the edge.

Montesanti et al. [5] used draw-filing to generate a 0.1–0.2 mm chamfer on the KDP crystal for preventing edge chip-out during diamond turning of large KDP crystal plane. But, there is no requirement for surface quality. To the best knowledge of the authors, there are no literatures on ultraprecision edge chamfering of KDP crystal in the order of millimeter.

Ultraprecision chamfering of KDP crystal is a challenge task as it is a kind of soft and brittle material. Compared with the commonly used materials, e.g., high speed steel, alumina, and silicon carbide, KDP crystal has much lower hardness and fracture toughness [6]. For materials with lower fracture toughness, it has lower ability to resist fracture, making its machining difficult as the materials tend to be removed in the brittle fracture mode. Furthermore, as a soft material, the machining chips are easy to be embedded in the machined surface, undermining the quality of the machined surface. To achieve the above-mentioned extremely high surface quality

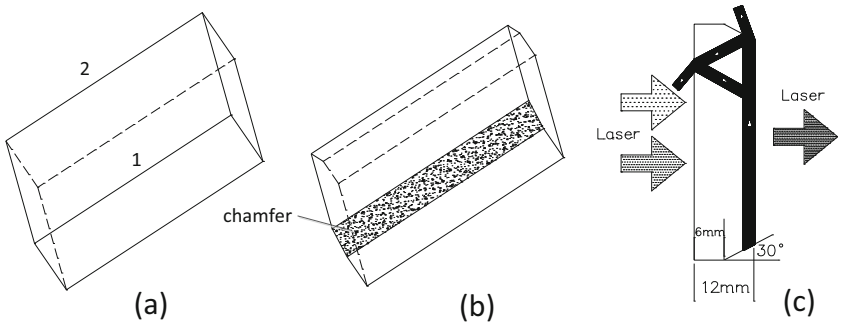


**Fig. 1** **a** Original KDP crystal. **b** Chamfered KDP crystal. **c** The dimension of chamfer [4]

on KDP crystals, several machining methods have been studied, including single point diamond turning (SPDT) [7–12], fly cutting [13–15], precise milling [9], grinding [16], magnetorheological finishing [17, 18], polishing [19, 20], ultrasonic vibration-assisted machining [21], and rotary ultrasonic machining [6]. KDP crystal was early machined using SPDT by controlling the machining parameters to achieve ductile machining [22]. However, due to the changing cutting direction of SPDT and the material anisotropy [8], the quality of the machining surface is non-uniform. To reduce the influence of the material anisotropy, fly cutting is usually applied to the machining of KDP crystal as the cutting direction is slightly changed.

Large size chamfering of KDP crystal may be achieved by fly cutting by treating the edges as small flat surfaces. However, for chamfers in the order of millimeter, the machining efficiency, which is measured as the machining time required, is too low to be accepted as its depth of cut (DOC) is usually several microns. If large DOC is adopted, large edge cracks will be generated. Furthermore, the diamond tool may be damaged due to the generated large dynamic cutting force.

For the edge chamfering of the KDP crystal with large size, there are three difficulties to be solved: (1) the large edge cracks may be produced at the initial few passes of the chamfering, (2) surface roughness RMS should be less than 5 nm, and (3) high-efficiency machining is required. To overcome these difficulties, a hybrid machining method which combines precision grinding with fly cutting is proposed and a hybrid machine tool has been developed in this paper. In addition, experiments have been carried out to determine the optimal machining procedures and verify the effectiveness of the proposed method.

## 2 Principle for crackless and high-efficiency ultraprecision chamfering of KDP crystal

### 2.1 Machining of KDP crystal without generating edge cracks

KDP crystal is a soft brittle material with strong anisotropy in terms of physical and mechanical properties. As revealed in the indentation experiments [23, 24], two major types of cracks, i.e., median crack and lateral crack, will be generated in the subsurface if the indentation depth is large than a critical value. Thus, the brittle material tends to be removed in brittle fracture mode.

When KDP crystal is chamfered by fly cutting or precision grinding as shown in Fig. 2a, b, respectively, it can be simplified as a single-edge orthogonal process as shown in Fig. 3, in which the cutting tool can be a diamond tool or a grinding grain. The critical DOCs of the KDP crystal on (001) crystal

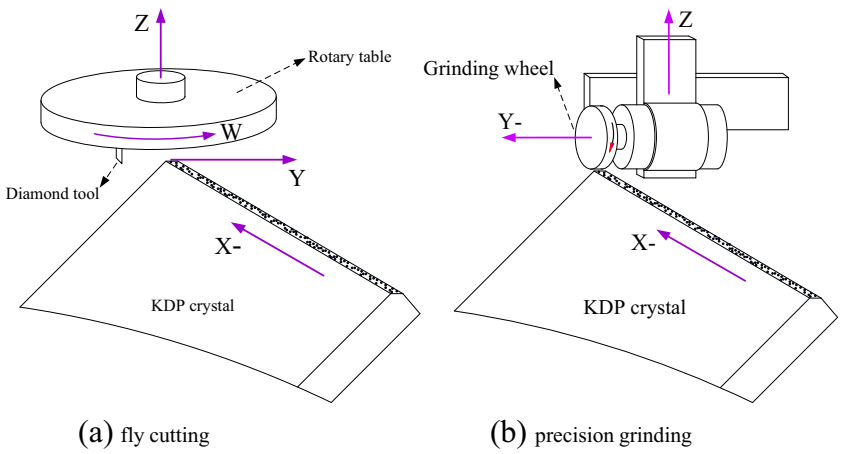


**Fig. 2** Schematic diagram for chamfering of KDP crystal. **a** Fly cutting. **b** Precision grinding

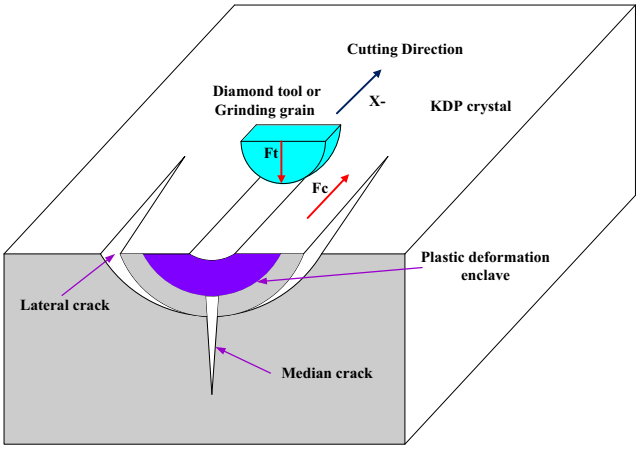


**Fig. 3** The crack systems in single-edge non-overlapping cut with cutting velocity normal to the shown plane of cross section [26]

plane, below which no crack will be generated, are 0.22 ±0.05, 0.53±0.06, and 0.23±0.05 μm when it is processed along (100), (110), and (120) crystallographic orientation, respectively [25]. If the DOC is larger than the critical DOC, median and lateral cracks will be generated as shown in Fig. 3. The median cracks produce subsurface damage, while the lateral cracks determine the removal of material in the form of hemi-spherical packets from the bulk material [26]. The size of the removed hemi-spherical packet is determined both by the thrust force $F_t$ and the cutting force $F_c$. The thrust force and the fracture toughness determine the width of the lateral crack and the depth of the median crack. For the same cutting force $F_c$, the larger the structural stiffness along the cutting direction, the smaller the size of the crack.

In chamfering of KDP crystal, if the cutting direction is perpendicular to its edge, large crack, which is much larger that induced by the same $F_c$ and $F_t$ in plane cutting, may be generated at the edge as the structural stiffness of the KDP crystal is relatively small. Such large-sized cracks are named as edge crack in this paper. When precision grinding is used in the chamfering of the KDP crystal, grinding direction should be along X direction as show in Fig. 2b to avoid the generation of the edge cracks as the structural stiffness along X direction is much larger than that along Y direction. When fly cutting is used in the chamfering of the KDP crystal, the KDP crystal can be fed in either along X or Y direction as shown in Fig. 4. When the KDP crystal is fed along X direction as shown in Fig. 4b, the cutting direction is along Y direction whose structural stiffness is small and thus edge cracks are easy to be generated. When the KDP crystal is fed along Y direction as shown in Fig. 4a, the cutting direction is varying. Edge cracks are easier to be generated at the two ends of the edge than at the middle of the edge as the perpendicular component of the cutting force at the two ends of the edge is much larger than that at the middle of the edge. Comparatively, fly cutting with the KDP crystal fed along Y direction is preferred as its machining time is shorter than that along X direction.

## 2.2 High-efficiency machining of KDP crystal

Although fly cutting is able to achieve high surface quality (roughness: RMS <5 nm), its machining efficiency is very low. The total DOC in fly cutting of large-sized KDP crystal surface, including the rough, semi-finish, and finish processes, is around 0.3 mm, the feed rates of the rough and finish fly cutting are 15~20 and 1~2 mm/min, respectively [5, 12, 27]. Thus, when fly cutting is used in chamfering of the two edges of the KDP crystal, because of the total DOC is about 3 mm, its machining time is even much longer than that of the flat surface.

To reduce the machining time and thus improve the machining efficiency, precision grinding as shown in Fig. 2b, in which the rotation direction is the same as the moving direction of the KDP crystal, is proposed to realize the high-efficiency machining of the KDP crystal without generating large edge cracks [28]. Due to the machining with multiple

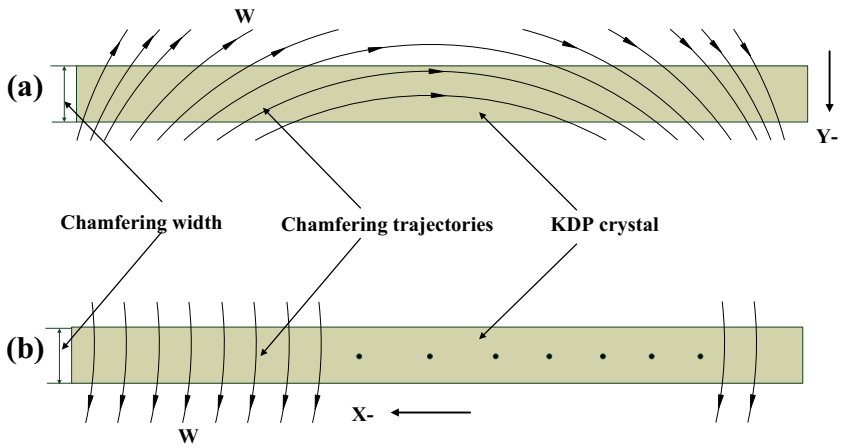


**Fig. 4** Trajectories of the fly cutting when the KDP crystal is fed. **a** Along Y direction. **b** Along X direction

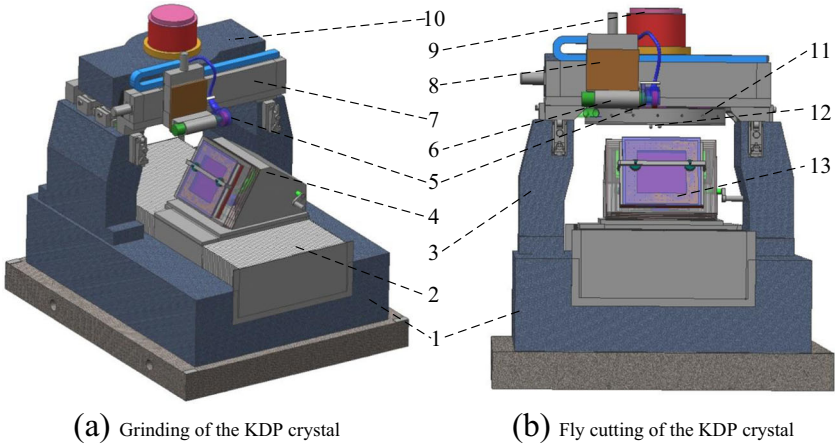


**Fig. 5** Machine setup for chamfering of the KDP crystal

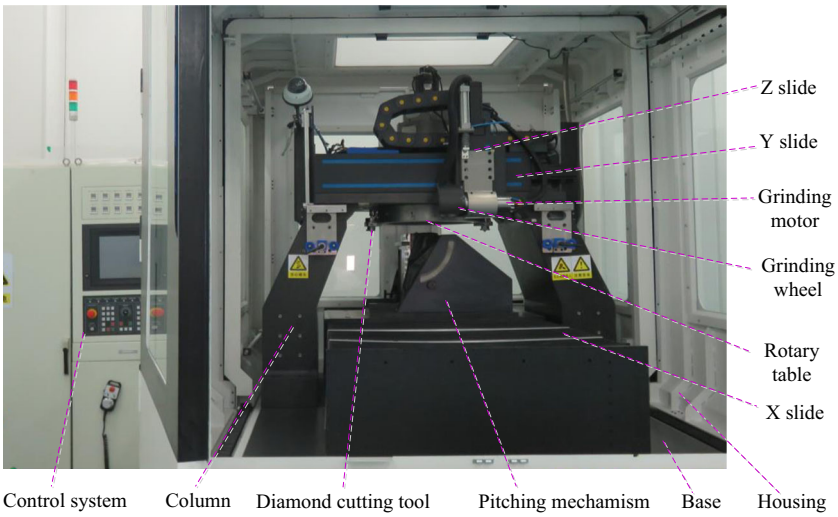


**Fig. 6** Photo of the combined machine tool for chamfering of KDP crystal

grinding grains and thus multiple cutting edges, the feed rate can be as high as 500 mm/min and machining efficiency can be raised by 50 times for the same DOC as that of fly cutting. Nevertheless, precision grinding may also cause problems, such as relatively low surface quality and shed grinding grains which may be embedded in the machined surface [16, 29].

### 2.3 A hybrid method for chamfering of KDP crystal

From the above analysis, it is known that fly cutting can ensure the high surface quality but its machining efficiency is too low, while precision grinding is characterized as high-efficiency machining with relatively low machined surface quality. Therefore, a new method is proposed in this paper

**Table 1** Experimental parameters

| Experimental equipment | Combined precision grinding–fly cutting machine tool | |
|---|---|---|
| Workpiece | Material | KDP crystal |
| | Size | 100 mm × 100 mm × 20 mm |
| Grinding wheel | CBN 1A1/T2 120/140 × 125 × 20 × 15 × 5 (granularity: 120/140, diameter: 125 mm, width: 20 mm, inner hole: 15 mm, thickness of machined layer: 5 mm) | |
| Fly cutting tool | SCD (rake angle: −45, tool nose radius: 5 mm, roughness of the rake face and flank face: 1 nm, edge radius: 60 nm, waviness of the cutting edge profile within 10: 200 nm) | |
| Grinding wheel rotation direction | Same as the feeding direction of the workpiece | |

**Table 2** Experiments on the effect of the feeding direction on edge cracking

| | Feeding direction | Grinding velocity (m/s) | Fly cutting velocity (m/s) | Velocity in X direction (mm/min) | Velocity in Y direction (mm/min) | Depth of cut (μm) |
|---|---|---|---|---|---|---|
| Grinding | Y | 18 | – | 20 | 500 | 15 |
| | X | 18 | – | 500 | 0 | 15 |
| Fly cutting | Y | – | 9 | – | 15 | 20 |
| | X | – | 9 | 15 | – | 20 |

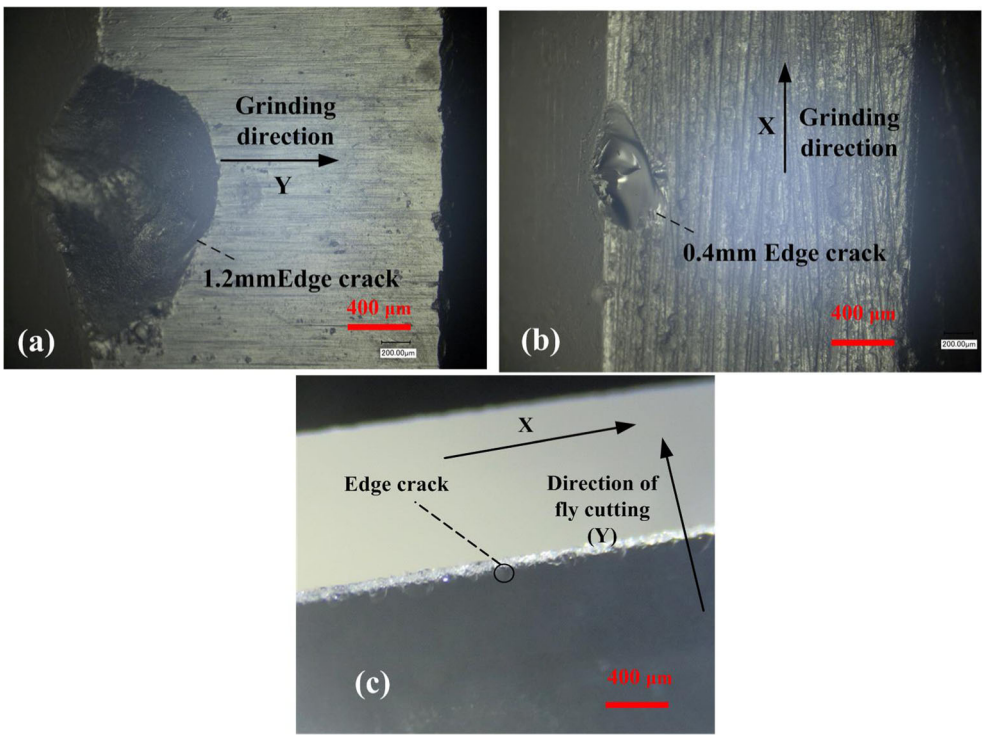


**Fig. 7** Microscopic images of the chamfered surface. **a** Edge crack generated by grinding in Y direction. **b** Edge crack generated by grinding in X direction. **c** Edge crack generated by fly cutting in Y direction

for chamfering of KDP crystal by combining precision grinding with fly cutting. The precision grinding is used to remove large amount of materials, while fly cutting is used to remove the cracks and other machining deficiencies generated by precision grinding and obtain high machined surface quality.

Based on the proposed method, a specialized machine tool, which combines the precision grinding with the fly cutting, for chamfering of the KDP crystal was developed as shown in Fig. 5. The machine tool must be designed and optimized to ensure high static and dynamic performance, which determines the machined surface quality [13, 30]. It consists of a base, column, X slide, Y slide, Z slide, vertical spindle, grinding axis, grinding wheel, pitching mechanism, rotary table, and other driving units. The combined machine tool adopts gantry structural configuration, which is closed frame and has symmetric structure, to improve the rigidity of the machine tool and reduce thermal deformation. The base of the machine tool adopts granite with low temperature sensitivity, which is helpful to improve the stability of the machine tool. The X slide consists of an aerostatic bearing guide with linearity of 0.1 μm/100 mm and a linear motor to achieve linear feeding with high precision and high dynamic performance. It is able

**Table 3** Experiments on the effect of grinding depth on edge cracking

| Edge no. | 1 | 2 | 3 | 4 | 5 | 6 | 7 | 8 |
|---|---|---|---|---|---|---|---|---|
| Depth of cut (μm) | 5 | 10 | 15 | 20 | 25 | 30 | 35 | 40 |
| Number of edge cracks (size >150 μm) | 0 | 2 | 8 | 18 | 28 | 35 | 42 | 55 |

**Table 4** Experiments on the effect of the depth of fly cutting on edge cracking

| Edge no. | 1 | 2 | 3 | 4 | 5 | 6 | 7 | 8 |
|---|---|---|---|---|---|---|---|---|
| Depth of cut (μm) | 3 | 5 | 8 | 10 | 20 | 30 | 35 | 40 |
| Number of edge cracks (size >150 μm) | 0 | 3 | 7 | 10 | 35 | 49 | 72 | 85 |

to achieve continuous stable feeding of the KDP crystal with feedrate as low as 1 mm/min. The vertical spindle is an aerostatic bearing spindle driven by a torque motor. Such configuration is helpful for reducing the spindle runout along axial and radial directions. The Y and Z axes are used for tool setting and feeding in precision grinding of the KDP crystal at different angles. The grinding axis uses aerostatic bearing to achieve high speed of the grinding wheel. The pitching mechanism is used to adjust the inclination angle of the edge of the KDP crystal within 0~60°. The developed machine tool is suitable for chamfering of the KDP crystal of size within 430 mm × 430 mm and chamfer angle within 0~60°.

Figure 5a shows the machine setup for grinding of the KDP crystal. The edge of the KDP crystal to be chamfered is parallel to the X slide, which is also schematically shown in Fig. 5. Figure 5b shows the machine setup for fly cutting of the KDP crystal, in which the edge of the KDP crystal to be machined is parallel to the Y slide. When the KDP crystal is fed along X slide, the trajectories of fly cutting are the same as that show in Fig. 4a. In this configuration, the time for fly cutting is reduced as the feeding distance of the X slide is reduced.

## 3 Experimental setup

To verify the effectiveness of the proposed method and determine the optimal machining procedure and parameters for the chamfering of the KDP crystal, series of machining experiments were carried out on the developed machine tool as shown in Fig. 6. The common experimental parameters are shown in Table 1. The size of the KDP crystal is 100 mm × 100 mm × 20 mm. The grinding wheel is CBN with good thermal conductivity and high hardness. Its rotation direction is the same as the feeding direction of the work piece. The fly cutting tool is single crystal diamond (SCD) with a nose radius of 5 mm and edge radius of 60 nm.

## 4 Results and discussions

### 4.1 Effects of the cutting parameters on edge cracking

#### *4.1.1 Effect of the feeding direction on edge cracking*

As the feeding direction affects the size of the edge cracks generated, experiments with the machining parameters as shown in Table 2 were carried out for the initial few passes of the chamfering. The obtained chamfered faces were observed with an optical microscope and the corresponding microscopic images are shown in Fig. 7a–c. It can be seen that grinding with Y feeding direction tends to generate large edge cracks with size around 1.2 mm as shown in Fig. 7a, while the size of the generated edge crack for grinding with X feeding direction is much smaller, which is only around 0.4 mm as shown in Fig. 7b. It is consistent with the result predicted in section 2.1 based on the fact that the structural stiffness along X direction (direction perpendicular to the edge) is much smaller than that along Y direction (direction in parallel to the edge), especially for the initial few passes.

For fly cutting with X and Y feeding direction, it has been found that the size and number of edge cracks generated with the same machining parameters are almost the same. As analyzed in section 2.1, for fly cutting with X feeding direction, the cutting direction is along the direction perpendicular to the edge. Therefore, edge cracks tend to be generated as the structural stiffness is small along the perpendicular direction. For fly cutting with Y feeding direction, the cutting direction is varying at different location of the edge. However, there is still a large component of cutting force along the perpendicular direction. This component will still induce edge cracks, which is probably the reason why the edge cracks for the two cases are almost the same. The edge cracks generated by fly cutting with Y feeding direction are shown in Fig. 7c.

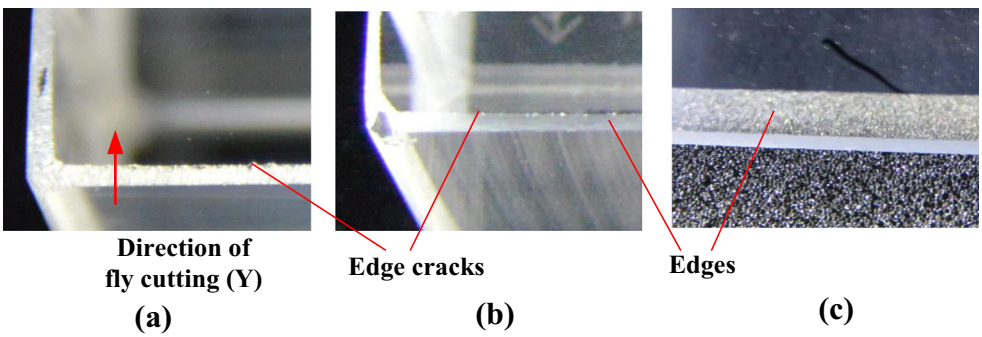


**Fig. 8** Edge cracks generated by fly cutting with different depth of cut. **a** 40 μm. **b** 20 μm. **c** 3 μm

*4.1.2 Effect of the grinding depth on edge cracking*

To investigate the effect of the grinding depth on edge cracking, experiments on grinding in X direction with machining parameters shown in Table 2 were carried out on the eight edges of the KDP crystal with the grinding depths shown in Table 3. The machined surfaces were observed with a microscope and the number of edge cracks with size larger than 150 μm were counted and listed in Table 3. It can be seen that there are no large edge cracks for grinding depth smaller than 10 μm. As the grinding depth increases, cracks tend to appear at the edge of the machined surface. In addition, the number of the edge cracks increases with the grinding depth, which is reasonable as the grinding force increases.

*4.1.3 Effect of the depth of fly cutting on edge cracking*

To investigate the effect of the depth of fly cutting on edge cracking, experiments on fly cutting in Y direction with machining parameters shown in Table 2 were carried out on the eight edges of the KDP crystal with the DOC shown in Table 4. The machined surfaces were observed with a microscope and the number of edge cracks with size larger than 150 μm were counted and listed in Table 4. The machined surfaces for edge no. 8, 5, and 1 are shown in Fig. 8a–c, respectively. It can be seen that there are no edge cracks when DOC is 3 μm, while the edge cracks and cutting marks can be clearly identified when DOC is 40 μm.

### 4.2 Analysis of the hybrid method for chamfering of KDP crystal

When the hybrid method is used for chamfering of KDP crystal, the critical issue to be dealt with is that the machining defects, e.g., cutting marks, surface cracks, and the shed grinding grains that are embedded in the machined surface, generated by grinding should be easily removed by the following fly cutting process. Therefore, combined experiments were carried out to investigate the machining defects.

Figure 9a shows the microscopic image of the machined surface by grinding in X direction with the machining parameters shown in Table 2. It can be seen that grinding marks can be obviously observed, which is probably due to the non-uniformity of the size of the grinding grains and the grinding chips that may be sliding between the grinding wheel and the machined surface. The machined surface was also measured by a white light interferometer. The obtained 3D surface profile is shown in Fig. 9b. It can be seen that the machined surface is filled with surface cracks, whose maximum size is around $0.2 \times 0.3$ mm and maximum depth around 20 μm.

In addition, the machined surface was thoroughly observed under the microscope to investigate whether any shed grinding grain was embedded in the machined surface. No grinding grains were found to be embedded in the machined surface, which may be explained as follows. Firstly, the hardness of the CBN grinding wheel is high with relatively large grinding grains (124 μm) and the grind depth is small. Secondly, due to the soft and easy deliquescence properties of the KDP crystal, many KDP powder were embedded in the surface of the grinding wheel. Thirdly, compressed air was applied to the grinding wheel which will blow off the shed grinding grains. Furthermore, if the shed grains are embedded in the machined surface, they may damage the cutting edge of the diamond

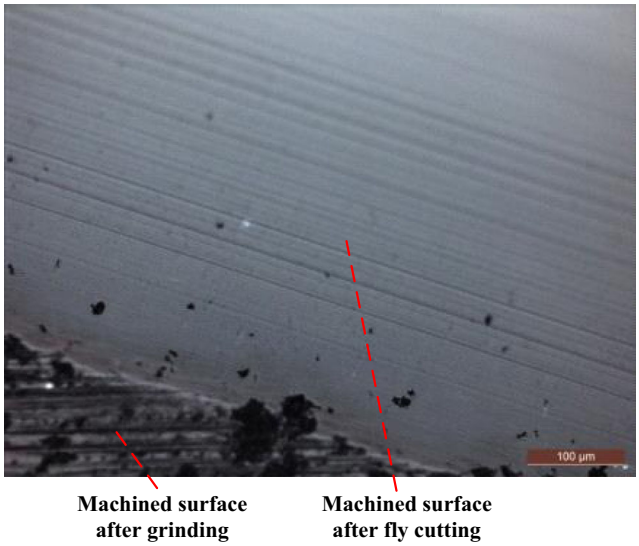


**Fig. 10** Microscope image of the machined surface after grinding and semi-finish fly cutting

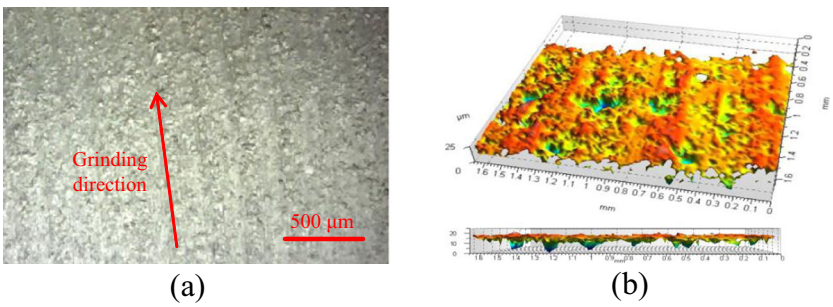


**Fig. 9** Surface profile of the surface after grinding. **a** Microscope image. **b** 3D profile

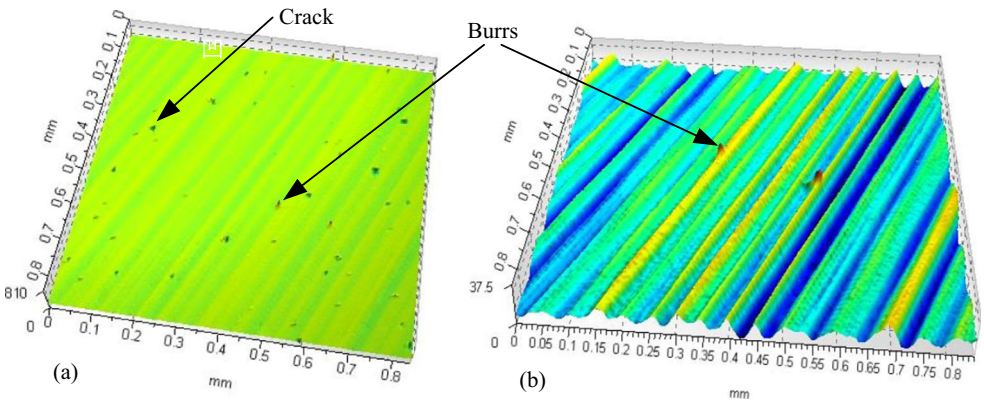


**Fig. 11** 3D surface profile. **a** Initial fly cutting. **b** Finish fly cutting

tool in the following fly cutting process. Therefore, the flank surface of diamond cutting tool was observed before and after cutting of the surface obtained by grinding. From the microscope image of the flank face of the diamond cutting tool after fly cutting, it can be seen that the diamond cutting keeps almost unchanged, which indirectly verifies that the shed grinding grains were not embedded in the machined surface.

Figure 10 shows the microscope image of the machined surface after grinding and semi-finish fly cutting. It can be seen that the surface quality was greatly improved after fly cutting, but there are clear cutting marks on the machined surface when large feedrate was adopted. There are no cutting marks after finish fly-cutting.

However, another two phenomena were observed during the experiments. Firstly, when the depth of the crack generated by grinding was 20 μm and fly cutting was applied to remove a total depth of 20 μm of material, small cracks with depth around 5~10 μm were still detected as shown in Fig. 11a. Secondly, many spikes with height around 20~150 μm were detected on the surface after fly cutting as shown in Fig. 11a. The first phenomenon may be explained as follows. Firstly, the grinding depth measured by white light interferometer may be smaller than the actual one due to its limitation in measuring cracks with steep inclination. Secondly, the depth of the brittle fractures corresponding to the surface cracks may be extended due to the machining force of the fly cutting. When the total DOC was increased to 60 μm, the surface cracks disappeared as shown in Fig. 11b. However, the spikes still existed on the machined surface by finish fly cutting. Part of these spikes was able to be wiped away. Thus, these spikes are probably the brittle fracture chips, which were generated at the entry of each pass due to the sharp edge of the KDP crystal and sticked to the machined surface to form the spikes. Therefore, the sharp edge of the KDP crystal was smoothed by polishing before finish fly cutting, by which the spikes

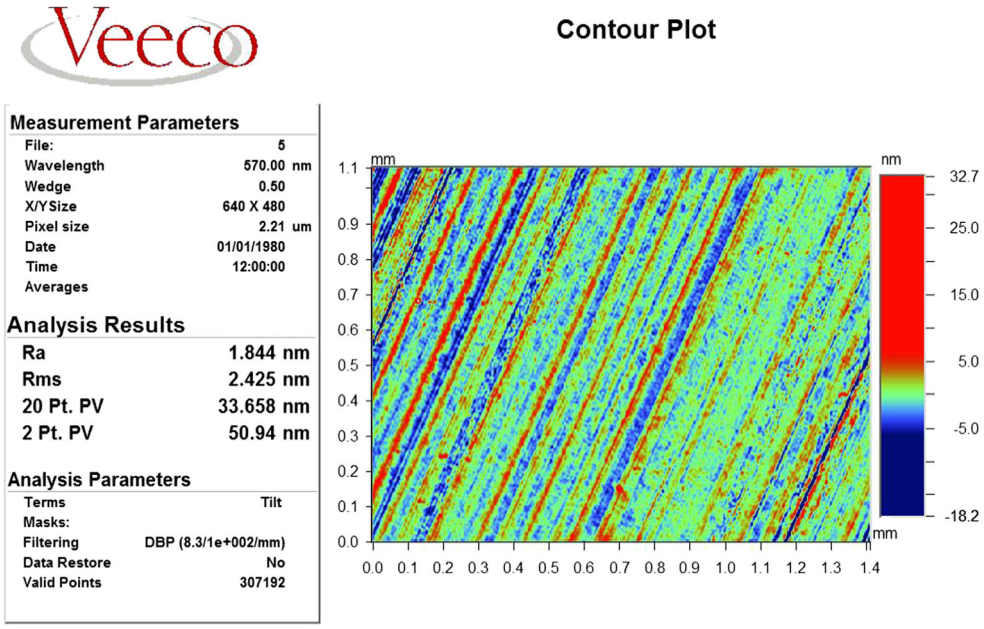


**Fig. 12** Surface roughness of the chamfered edge surface

**Table 5** Machining parameters and time for chamfering of the KDP crystal using fly cutting

| | 1st initial fly cutting | 2nd initial fly cutting | 3rd initial fly cutting | Semi-finish fly cutting | Finish fly cutting |
|---|---|---|---|---|---|
| DOC (μm) | 3 | 15 | 10 | 6 | 4 |
| Workpiece feedrate (mm/min) | 10 | 15 | 10 | 4 | 2 |
| Total DOC (μm) | 50 | 2640 | 20 | 6 | 4 |
| No. of passes | 17 | 176 | 2 | 1 | 1 |
| Machining time (min) | 18.7 | 129 | 2.2 | 2.75 | 5.5 |
| Auxiliary time (min) | 68 | 704 | 8 | 4 | 4 |
| Total time (min) | 946.15 | | | | |

totally disappeared. Finally, surface roughness of about Rms 2.4 nm as shown in Fig. 12 was achieved. Such surface quality is comparable to that obtained in the plane processing of KDP crystal in literature, e.g., 1.3–1.7 nm in [7], 2.4 nm in [13], 1–3 nm in [5].

### 4.3 Efficiency of the hybrid method for chamfering of KDP crystal

To verify the efficiency of the hybrid method for chamfering of KDP crystal, a series of experiments were carried out by fly cutting and the hybrid method. We determined the optimal machining procedure and parameters for chamfering. The length of the KDP crystal is 100 mm and the total DOC is 2720 μm. The machine setup is shown in Fig. 5. The machining parameters and the corresponding machining time are listed in Tables 5 and 6, respectively. The auxiliary time is the time taken for retraction of the KDP crystal and feeding of the cutting tool between each passes, which is 4 min in average. It can be seen from Tables 5 and 6 that the total machining time for fly cutting is 946.15 min, while the machining by the hybrid method is only 153.65 min for the same machined surface quality. Therefore, the machining efficiency of the hybrid method is improved by about five times.

## 5 Conclusions

A hybrid method, which combines precision grinding with fly cutting, is proposed for crackless and high-efficiency ultraprecision chamfering of KDP crystal in this study. In addition, a combined machine tool has been developed and experiments have been carried out on it to determine the optimal machining procedures and verify the effectiveness of the proposed method. The following conclusions can be drawn from this study:

1. Edge cracks tend to be generated at the initial few passes of chamfering. Grinding along the edge direction of the KDP crystal is helpful in reducing the size of the edge cracks. The optimal machining parameters for eliminating edge cracks larger than 150 μm are as follows: grinding depth 5 μm and DOC for fly cutting 3 μm when the feedrate for grinding and fly cutting are 500 and 10 mm/min, respectively.
2. The material removal for grinding is in brittle-mode accomplished by propagation of cracks due to brittle fracture. The machined surface by grinding is filled with machining defects, including surface cracks with depth around 20 μm and cutting marks. The machining defects can be removed by fly cutting, and high machined surface quality with surface roughness of 2.4 nm has been obtained.

**Table 6** Machining parameters and time for chamfering of the KDP crystal using the hybrid method

| | Initial grinding | Rapid grinding | Finish grinding | Initial fly cutting | Semi-finish fly cutting | Finish fly cutting |
|---|---|---|---|---|---|---|
| DOC (μm) | 5 | 15 | 5 | 10 | 6 | 4 |
| Workpiece feedrate (mm/min) | 500 | 500 | 500 | 10 | 4 | 2 |
| Total DOC (μm) | 50 | 2500 | 100 | 60 | 6 | 4 |
| No. of passes | | | | 6 | 1 | 1 |
| Machining time (min) | 2.2 | 36.8 | 4.4 | 6.6 | 2.75 | 5.5 |
| Auxiliary time (min) | – | – | – | 24 | 4 | 4 |
| Tool retracting time (min) (500 mm/min feedrate) | 2.2 | 36.8 | 4.4 | – | – | – |
| Total time (min) | 153.65 | | | | | |

3. Fly cutting is too time-consuming in chamfering of KDP crystal as the amount of materials to be removed is in the order of millimeter. The machining efficiency can be improved by nearly five times using the hybrid method to produce the same machined surface quality.

**Acknowledgments** The authors gratefully acknowledge the financial support of the national important science and technology project of China (grant number 2013 zx04006011).

## References

1. Paisner JA, Boyes JD (1994) National Ignition Facility would boost US industrial competitiveness. Laser Focus World 30:75
2. Lin Z, Deng X, Fan D, Wang S, Chen S, Zhu J, Qian L et al (1999) SG-II laser elementary research and precision SG-II program. Fusion Eng Design 44:61–66, http://dx.doi.org/10.1016/S0920-3796(98)00308-1
3. Novikov VN, Belkov SA, Buiko SA, Voronich IN, Efimov DG, Zaretsky AI, Kochemasov GG et al (1999) Transverse SRS in KDP and KD*P crystals. Proc SPIE 3492:1009–1018
4. Barker CE, Sacks RA, Van Wonterghem BM, Caird JA, Murray JR, Campbell JH, Kyle KR et al (1995) Transverse stimulated Raman scattering in KDP. Proc SPIE 2633:501–505
5. Montesanti RC, Thompson SL A procedure for diamond turning KDP crystals[R]. (1995) Lawrence Livermore National Laboratory UCRL-ID-121651
6. Wang Q, Cong W, Pei ZJ, Gao H, Kang R (2009) Rotary ultrasonic machining of potassium dihydrogen phosphate (KDP) crystal: an experimental investigation on surface roughness. J Manuf Process 11:66–73, http://dx.doi.org/10.1016/j.jmapro.2009.09.001
7. Tie G, Dai Y, Guan C, Zhu D, Song B (2013) Research on full-aperture ductile cutting of KDP crystals using spiral turning technique. J Mater Process Technol 213:2137–2144, http://dx.doi.org/10.1016/j.jmatprotec.2013.06.006
8. Zhao Q, Wang Y, Yu G, Dong S, Zhang X (2009) Investigation of anisotropic mechanisms in ultra-precision diamond machining of KDP crystal. J Mater Process Technol 209:4169–4177, http://dx.doi.org/10.1016/j.jmatprotec.2008.10.010
9. Chen M, Pang Q, Wang J, Cheng K (2008) Analysis of 3D microtopography in machined KDP crystal surfaces based on fractal and wavelet methods. Int J Mach Tools Manuf 48:905–913, http://dx.doi.org/10.1016/j.ijmachtools.2007.11.002
10. Xu Q, Wang J, Li W, Zeng X, Jing S (1999) Defects of KDP crystal fabricated by single-point diamond turning. Proc SPIE 3862:236–239
11. Namba Y, Katagiri M, Nakatsuka M (1998) Single point diamond turning of KDP inorganic nonlinear optical crystals for laser fusion. J Japan Soc Precision Eng 64:1487–1491
12. Fuchs BA, Hed PP, Baker PC (1986) Fine diamond turning of KDP crystals. Appl Opt 25:1733–1735. doi:10.1364/AO.25.001733
13. Chen W, Liang Y, Sun Y, Huo D, Lu L, Liu H (2014) Design philosophy of an ultra-precision fly cutting machine tool for KDP crystal machining and its implementation on the structure design. Int J Adv Manuf Technol 70:429–438. doi:10.1007/s00170-013-5299-9
14. Liang Y, Chen W, Bai Q, Sun Y, Chen G, Zhang Q, Sun Y (2013) Design and dynamic optimization of an ultraprecision diamond flycutting machine tool for large KDP crystal machining. Int J Adv Manuf Technol 69:237–244. doi:10.1007/s00170-013-5020-z
15. Liang Y, Chen W, Sun Y, Luo X, Lu L, Liu H (2014) A mechanical structure-based design method and its implementation on a fly-cutting machine tool design. Int J Adv Manuf Technol 70:1915–1921. doi:10.1007/s00170-013-5436-5
16. Namba Y, Katagiri M (1999) Ultraprecision grinding of potassium dehydrogen phosphate crystals for getting optical surfaces. Proc SPIE 3578:692–693
17. Jacobs SD (2007) Manipulating mechanics and chemistry in precision optics finishing. Sci Technol Adv Mater 8:153
18. Arrasmith SR, Kozhinova IA, Gregg LL, Shorey AB, Romanofsky HJ, Jacobs SD, Golini D et al (1999) Details of the polishing spot in magnetorheological finishing (MRF). Proc SPIE 3782:92–99
19. Ramaswamy V, Divino MD (1972) An Apparatus for Polishing Water Soluble Crystals. Rev Sci Instrum 43:1294–1296, http://dx.doi.org/10.1063/1.1685907
20. Gao H, Wang B, Guo D, Li Y (2010) Experimental Study on Abrasive-Free Polishing for KDP Crystal. J Electrochem Soc 157:H853–H856. doi:10.1149/1.3458869
21. Zhang J, Wang D, Feng P, Wu Z, Zhang C (2015) Material Removal Characteristics of KDP Crystal in Ultrasonic Vibration-Assisted Scratch Process. Mater Manuf Process. doi:10.1080/10426914.2015.1070423
22. Blake PN, Scattergood RO (1990) Ductile-Regime Machining of Germanium and Silicon. J Am Ceram Soc 73:949–957
23. Marshall DB, Lawn BR, Evans AG (1982) Elastic/plastic indentation damage in ceramics: the lateral crack system. J Am Ceram Soc 65:561–566
24. Lu C, Gao H, Wang B, Guo D, Teng X, Kang R, Wu D (2010) Experimental study of single-tip scratching on potassium dihydrogen phosphate single crystal. J Mechanical Eng 46:179–185
25. Lu C, Gao H, Wang B, Wang Q (2009) Anisotropic Analysis on Processed Surface of KDP Single Crystals. Adv Mater Res 76-78:223–228
26. Arif M, Xinquan Z, Rahman M, Kumar S (2013) A predictive model of the critical undeformed chip thickness for ductile–brittle transition in nano-machining of brittle materials. Int J Mach Tools Manuf 64:114–122, http://dx.doi.org/10.1016/j.ijmachtools.2012.08.005
27. Peng YF, Guo YB, Xu Q. Influence of cutting velocity on surface roughness of KDP: 4th International Symposium on Advanced Optical Manufacturing and Testing Technologies: Advanced Optical Manufacturing Technologies, 2009[C].
28. Chen X, Rowe WB, Cai R (2002) Precision grinding using CBN wheels. Int J Mach Tools Manuf 42:585–593, http://dx.doi.org/10.1016/S0890-6955(01)00152-3
29. Pei ZJ, Strasbaugh A (2001) Fine grinding of silicon wafers. Int J Mach Tools Manuf 41:659–672, http://dx.doi.org/10.1016/S0890-6955(00)00101-2
30. Chen W, Liang Y, Luo X, Sun Y, Wang H (2014) Multi-scale surface simulation of the KDP crystal fly cutting machining. Int J Adv Manuf Technol 73:289–297. doi:10.1007/s00170-014-5748-0